

PACS numbers: 42.65.Hw; 42.65.Tg; 42.70.Nq; 42.40.Eq
DOI: 10.1070/QE2011v041n11ABEH014660

Optical surface wave in a crystal with diffusion photorefractive nonlinearity

S.A. Chetkin, I.M. Akhmedzhanov

Abstract. **We consider a steady-state nonlinear photorefractive surface wave (PR SW) with TE or TM polarisation when the refractive index of the photorefractive crystal (PRC) depends on the strength of the diffusion crystal electric field emerging upon the wave propagation. We have determined the phase trajectory and transverse structure of the PR SW intensity distribution for different values of the diffusion photorefractive nonlinearity. We have investigated a photorefractive diffraction grating, which arises in the surface PRC layer during propagation of the nonlinear PR SW.**

Keywords: *photorefractive crystal, photorefractive nonlinear surface wave, diffuse crystal field.*

1. Introduction

In a photorefractive crystal (PRC), distribution of a photoinduced electric charge in the plane, perpendicular to the trajectory of the light beam, repeats distribution of its intensity, which causes local changes in the PRC electric field and refractive index [1–4]. The PRC becomes locally inhomogeneous, its optical density in the vicinity of the beam trajectory changes, which is accompanied by either scattering or focusing, or bending of the beam. In the case of interference of coherent beams in a polarised PRC (when one of the beams arises due to scattering of the other, for example, by random inhomogeneities), photorefractive self-action leads to the appearance of a Bragg diffraction grating, repeating the structure of the interference pattern, but differing from it in phase [2]. The interfering beams exchange energy on such a grating, the energy being transferred in the direction that is opposite to the direction of the crystal polarisation [1–3]. As a result, when the laser beam propagates along the PRC face that is perpendicular to the optical axis, there emerges a nonlinear photorefractive surface wave (PR SW) [5–8].

Current trends in nanominiaturization of optoelectronic devices have rekindled interest in nonlinear optical phenomena for which optical radiation concentrates, and its spatial, temporal and spectral characteristics change in a controllable manner. In this connection, of interest is to study the experimentally discovered [9] channelling and diffractionless propagation of the laser beam at the interface between two media, one of which is photorefractive.

In this paper, we have investigated the steady-state propagation equation for TE- and TM-polarised nonlinear PR SWs in the PRC with a nonlinear dependence of the 'diffuse' refractive index on the intensity. We have determined the form of the phase trajectory and the intensity distribution for the nonlinear PR SW at different values of the photorefractive diffusion nonlinearity. We have also studied the photorefractive grating arising in the surface PRC layer during the propagation of the nonlinear PR SW.

S.A. Chetkin, I.M. Akhmedzhanov A.M. Prokhorov General Physics Institute, Russian Academy of Sciences, ul. Vavilova 38, 119991 Moscow, Russia; e-mail: chetkin@kapella.gpi.ru, eldar@kapella.gpi.ru

Received 30 May 2011; revision received 14 October 2011
Kvantovaya Elektronika **41** (11) 980–985 (2011)
Translated by I.A. Ulitkin

2. Propagation of light in a surface region of the nonlinear PRC

By the example of single crystal strontium barium niobate $Sr_{0.6}Ba_{0.4}NbO_3$ (SBN), we consider the steady-state nonlinear PR SW in a polarised uniaxial PRC. We assume that due to the diffusion of photoinduced electrical charges, the refractive index of the PRC in the direction of intensity gradient [1–3] is nonlinear and inhomogeneous. The geometry of the problem is illustrated in Fig. 1: the PRC occupies the region $x > 0$; its optical axis is parallel to the x axis; the linearly polarised light beam is incident on the PRC face at an angle exceeding the angle of total internal reflection (in SBN for the ordinary and extraordinary waves, it is equal to 25.63 and 25.79 deg, respectively). Under these conditions, propagation of monochromatic TE and TM light waves in the PRC is described by the equations [10–12]

$$\Delta \boldsymbol{E} + k^2 \boldsymbol{E} - \nabla(\nabla \boldsymbol{E}) = 0, \ \Delta \boldsymbol{H} + k^2 \boldsymbol{H} + \varepsilon^{-1} \nabla\varepsilon \times \nabla \times \boldsymbol{H} = 0, \quad (1)$$

where $\varepsilon = \varepsilon(x, z)$ is the dielectric constant of the PRC (magnetic permeability $\mu = 1$); $k = 2\pi\varepsilon^{1/2}(x, z)/\lambda$; λ is the wavelength of light in vacuum. Propagation of light in the PRC is accompanied by the emergence of the crystal electric field E_x^{sc} [1–4], which, in the geometry of our problem, is directed along the optical axis of the PRC (Fig. 1). The PRC is uniaxial, but its refractive indices for waves with extraordinary ($n_{||}$) and ordinary ($n_{||}$) polarisations change [10–12]:

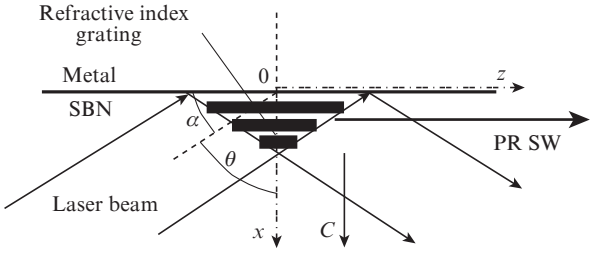

Figure 1. Excitation of the nonlinear PR SW by a laser beam in the SBN crystal and emergence of a photorefractive phase diffraction grating in the region of interference between incident and reflected laser beams; C is the optical axis of the crystal.

$$n_{\|} = n_e - n_e^3 r_{33} E_x^{sc}/2, \quad n_{\perp} = n_o - n_o^3 r_{13} E_x^{sc}/2, \tag{2}$$

where r_{33} and r_{13} are the electro-optic tensor components. In the absence of a dc field, when the light is incident at an angle θ to the optical axis, the refractive index for the ordinary wave is constant, $n_{\perp}^{o}(\theta) = n_o$, whereas for the extraordinary wave it can be written as [10–12]

$$n_{\|}^{e}(\theta) = \frac{n_{\perp} n_{\|}}{[(n_{\|}\cos\theta)^2 + (n_{\perp}\sin\theta)^2]^{1/2}}. \tag{3}$$

The influence of the field E_x^{sc} on the refractive indices of ordinary and extraordinary beams is taken into account by substituting (2) into (3). The wave propagates in the xz plane along the axis z, and the dielectric constant varies only along the x axis. The medium along the z axis is uniform, and so the component of the wave amplitude, which depends on the coordinate z, is chosen proportional to $\exp(i\beta z)$ [12], where β is the propagation constant.

Because in the uniaxial PRC the linearly polarised light has two independent polarisations, then for the TE wave (the component E_y of the electric field amplitude vector is nonzero) and TM wave (the component H_y of the magnetic field strength amplitude vector is also nonzero), equations (1) take the form [11, 12]:

$$\frac{\partial^2 E_y}{\partial x^2} + \left(\frac{\varepsilon_{\perp}\omega^2}{c^2} - \beta^2\right) E_y = 0,$$

$$\frac{\partial}{\partial x}\left[\frac{1}{\varepsilon_{\|}(\theta)}\frac{\partial H_y}{\partial x}\right] + \left[\frac{\omega^2}{c^2} - \frac{\beta^2}{\varepsilon_{\|}(\theta)}\right] H_y = 0. \tag{4}$$

When the inequalities

$$\frac{d}{dx}\left(\frac{1}{\sqrt{\varepsilon_{\|}\omega^2/c^2 - \beta^2}}\right) \ll 1, \quad \sqrt{\varepsilon_{\|}}\frac{d^2}{dx^2}\left(\frac{1}{\sqrt{\varepsilon_{\|}}}\right) \ll \frac{\omega^2}{c^2} - \beta^2$$

are fulfilled, using the expression $H_y(x) = \sqrt{\varepsilon_{\|}(x)}U(x)$ equations (4) for $U(x)$ and $E_y(x)$ are reduced to the same form [11]. Components of the electric (magnetic) field amplitude vector of the TE (TM) wave, which lie in the plane of incidence, are obtained from Maxwell's equations:

$$H_x = \frac{\beta E_y}{\omega}, \quad H_z = \frac{i}{\omega}\frac{\partial E_y}{\partial x}, \quad E_x = -\frac{\beta H_y}{\omega}, \quad E_z = -\frac{i}{\omega}\frac{\partial H_y}{\partial x}. \tag{5}$$

In the case of diffusion redistribution of photoinduced charge carriers, the crystal field E_x^{sc} in the PRC is given by [1–4]

$$E_x^{sc} = -\frac{k_B T\, \partial I_{TE,TM}/\partial x}{e(I_{TE,TM} + I_d)}, \tag{6}$$

where $I_{TM} = Z_0|H_y|^2/(2n_{\|}) = n_{\|}U^2/(2c)$ and $I_{TE} = n_{\perp}|E_y|^2/(2Z_0)$ are the TE- and TM-wave intensities; Z_0 is the impedance of vacuum [13]; I_d is the 'dark' intensity of the PRC [1–3]; T is the temperature; e is the electron charge. Therefore, by substituting (2), (3), (6) into (4), the equations for the amplitudes of the TE and TM waves take the form

$$\frac{d^2}{dx^2}E_y(x) + 2k_0^2 n_{\perp}^4 r_{13}\frac{k_B T}{e}\frac{E_y^2(x)}{E_y^2(x) + 2I_d Z_0/n_{\perp}}\frac{d}{dx}E_y(x) + (k_0^2 n_{\|}^2 - \beta^2)E_y(x) = 0, \tag{7}$$

$$\frac{d^2}{dx^2}U(x) + 2k_0^2 n_{\|}^4 r_{33}\frac{k_B T}{e}\frac{U^2(x)}{U^2(x) + 2I_d/(n_{\|}Z_0)}\frac{d}{dx}U(x) + (k_0^2 n_{\|}^2 - \beta^2)U(x) = 0,$$

where k_0 is the wave number in vacuum. In dimensionless variables, equations (7) can be simplified, and their constituent parameters are independent.

Algebraic expressions for the scale factors of the field length, intensity and amplitude [14], consisting of parameters $r_{33,13}$, k_0, e, c, for TE- and TM-polarised nonlinear PR SWs in the SI system have the form

$$x^*_{TE,TM} = \frac{e}{2k_0^2 n_{\perp,\|}^4 r_{13,33} k_B T}, \quad I_0^{TE,TM} = \frac{k_0^2 n_{e,o} ec}{r_{13,33}},$$

$$H_0 = \frac{n_{\|}E_0}{Z_0} = k_0 n_{\|}\sqrt{\frac{2e}{\mu_0 r_{33}}}, \quad E_0 = \sqrt{\frac{2Z_0 I_0}{n_{\perp}}} = k_0\sqrt{\frac{2e}{\varepsilon_0 r_{13}}},$$

and equations (7) transform into the equation

$$\frac{d^2 V}{du^2} + \frac{V^2}{V^2 + C^2}\frac{dV}{du} + QV = 0, \tag{8}$$

where $V = E/E_0$ or $(U/H_0)n_{\|}$ for TE or TM polarisations; $u = x/x^*$;

$$C^2_{TE,TM} = \frac{r_{13,33}I_d}{eck_0^2} = \frac{I_d}{I_0^{TE,TM}};$$

$Q_{TE,TM} = (n_{\perp,\|}P_{TE,TM}\cos\theta)^2$; $P_{TE,TM} = k_0 x^*$. Independent parameters C^2 and Q determine the amplitude and the depth of PR SW penetration, x^*, into the PRC. Equation (8) with the nonlinear damping factor $\gamma = V^2/(V^2 + C^2)$ determines the stationary distribution of the PR SW amplitude oscillating in the direction of the x axis. In the optically transparent PRC, damping γ is determined by the spatial redistribution of the PR SW energy in the direction, opposite to the that of the PRC polarisation, rather than by absorption. When $I \ll I_d$, the damping factor $\gamma \sim I/(2I_d) \sim V^2/(2I_d) \ll 1$ of the nonlinear PR SW is the quantity of the second order of smallness; therefore, in linearizing equation (8), it becomes an equation for the harmonic oscillator without damping. At high intensities ($\gamma \to 1$), expression (8) transforms into a linear equation with constant damping. In the intermediate range of intensities, the amplitude distribution in the PR SW cross section is described by the equation for an oscillator with nonlinear damping.

The coefficient Q in (8) has the meaning of the restoring force. It determines the square of the spatial oscillation frequency Ω of the nonlinear PR SW amplitude along the optical axis of the PRC:

$$\Omega^2 = \beta^2 - k_0^2 n_{\perp,\|}^2 + \left[\frac{k_0^2 n_{\perp,\|}^4 r_{33,13} k_B T I}{e(I + I_d)}\right]^2.$$

For SBN, $I_d \approx 0.03$ W cm^{-2} [15]; therefore, at $I \geqslant I_d$, the nonlinear equation (8) reduces to the linear:

$$\frac{d^2 V}{du^2} + \frac{dV}{du} + QV = 0. \tag{9}$$

The emergence of the nonlinear PR SW in the polarised PRC is due to the interference of two coherent beams, one of which is the result of reflection of the other from the PRC interface [5–9]. Specular reflection from the PRC face (coated with a metal film) that is required for the interference can

occur at any angles of incidence of the light beam. Specular reflection from the PRC face that is in contact with an optically less dense dielectric medium occurs in a limited range of angles exceeding the angle of total internal reflection. The boundary conditions are different for these two cases; however, in the corresponding solutions to equations (8), (9) the differences manifest themselves in the surface PRC layer of thickness, significantly smaller than the depth of the PR SW penetration $x^* = 1/\gamma$, in which the PR SW field is small. At depths $x \sim x^*$, the solutions corresponding to different boundary conditions will be qualitatively the same [5, 6, 9]. Without loss of generality, we consider the case of a metal-coated face of the PRC, for which boundary conditions have the form

$$V(u \to 0) = 0, \quad \frac{\mathrm{d}V(u \to 0)}{\mathrm{d}u} = G, \quad V(u \to -\infty) = 0.$$

Thus, solution of equations (8), (9) reduces to solution of the Cauchy problem for the spatial coordinate x, measured along the optical axis of the crystal [5–9]. The constant G is determined by the PRC nonlinearity. The solution of equation (9) has the form

$$V(u) = \frac{4G}{\sqrt{1-4Q^2}} \exp\left(-\frac{u}{2}\right) \sinh \frac{u\sqrt{1-4Q^2}}{2},$$

and at $Q = 1/2$

$$V(u) = uG \exp(-u/2).$$

The PR SW amplitude distribution in the PRC is determined by the parameter Q^2: at a real value of $\sqrt{1/4 - Q^2}$ in the cross section, it has the form of an aperiodic oscillation; at $1/4 - Q^2 = 0$, the wave has the form of an oscillation with critical damping and is localised in the narrowest PRC layer; at a complex value of $\sqrt{1/4 - Q^2}$ the PR SW amplitude distribution oscillates and decays along the x axis. At $Q \gg 1$, the nonlinear PR SW is not produced and we observe only interference of the incident and reflected beams. The value $Q = 0$ corresponds to the propagation of the nonlinear PR SW, parallel to the PRC boundary. In this case, the amplitude is constant across the beam cross section.

For quantitative estimates and the analysis of the correspondence of experimental data with the results of calculations, it is necessary to establish the relationship between the PR SW power W and the parameter G. For this purpose, we replace one of the boundary conditions by the normalisation condition:

$$W = \int_0^\infty I(x)\mathrm{d}x.$$

Then,

$$G^2 = \frac{W(1-2Q)}{x^* I_0}, \tag{10}$$

and the boundary conditions for the derivative of the field amplitude for the TE- and TM-polarised waves have the form

$$\left.\frac{\partial E_y}{\partial x}\right|_{x=0} = \sqrt{\frac{2Z_0 W(1 - 2n_\perp^2 k_0^2 x^{*2} \cos^2\theta)}{n_\perp x^{*3}}},$$

$$\left.\frac{\partial H_y}{\partial x}\right|_{x=0} = \sqrt{\frac{2n_\parallel W(1 - 2n_\parallel^2 k_0^2 x^{*2} \cos^2\theta)}{Z_0 x^{*3}}}. \tag{11}$$

Graphical representation of the PR SW amplitude distribution in the crystal is given by the phase trajectories [16] of equations (8), (9). The trajectories have the form of dependences of the derivatives of the electric (TE wave) and magnetic (TM wave) field amplitudes of the nonlinear PR SW on these amplitudes. As a parameter, we use the x coordinate, measured along the optical axis of the crystal. Depending on Q, for equation (9) there are three types of phase trajectories with the corresponding singular points that are positions of stable equilibrium: the centre if $\gamma = 0$ and $Q \gg 1$, stable focus if $Q > 1/2$, and stable node when the inverse inequality is fulfilled. At these points the PR SW amplitude and its derivative are equal to zero as the transverse coordinate tends to infinity. If the crystal occupies the half-space, it means that the optical radiation is localised at the surface. Thus, existence of a stable singular point at the origin of the phase plane coordinates implies existence of the nonlinear PR SW. The physical meaning of the singular point as the equilibrium position consists in the fact that the positively determined quadratic form of the energy density of the nonlinear PR SW $H^2 + E^2 \propto (\partial E/\partial x)^2 + E^2$ reaches its minimum, equal to zero.

3. Numerical study of the PNSW in the SBN

The nonlinear equation (8) was solved numerically by the Runge–Kutta fourth order method. In calculations the PRC orientation corresponded to that presented in Fig. 1; the angle α between the direction of light propagation and the PRC face, perpendicular to the optical axis, was 0.02 rad; the derivative $\partial H_y/\partial x|_{x=0}$ at the PRC boundary was equal to 10^5, 10^6, 10^7 and 10^{10}. The results of calculation of the amplitude distribution of nonlinear TE- and TM-polarised PR SWs are given in relative units, because the literature contains no clearly defined data about the dark intensity of the SBN. Figures 2a, b show the distribution of the components $H_y(x)$ of the magnetic field vector amplitude of the nonlinear TM-polarised PR SW for $\partial H_y/\partial x|_{x=0} = 10^6$ and 10^{10}. One can see the influence of diffusion photorefraction on localisation of radiation near the PRC surface. The distribution $H_y(x)$ has the form of a damped oscillation, whose spatial oscillation period depends on the PR SW intensity and angle α. When the nonlinearity (Fig. 2a) is weak, radiation penetrates into the PRC, experiencing slight damping (redistribution of the PR SW energy over the PRC cross section is negligible). The increase in $\partial H_y/\partial x|_{x=0}$ to 10^7 leads to an increase in photorefraction and is accompanied by an increase in radiation localisation, so that when $\partial H_y/\partial x|_{x=0} = 10^{10}$ (Fig. 2b), the depth of the PR SW localisation is 40–50 μm . In the steady state, the PR SW amplitude distribution does not change along the z axis, i.e., the PR SW has a stationary spectrum of spatial frequencies: the wider the spectrum, the more intense the photorefraction (Figs 2c, d). Figures 2e, f present the phase trajectories of nonlinear PR SWs. When the diffusion photorefraction is weak, the phase trajectory of the PR SW represents a limit cycle in the form of a circle (ellipse) ($\partial H_y/\partial x|_{x=0} = 10^5$). The linear oscillator with damping does not have such features [16]. With increasing diffusion photorefraction ($\partial H_y/\partial x|_{x=0} = 10^7$, Fig. 2e), the phase trajectory of the nonlinear PR SW transforms into a spiral, 'wound' on the limit cycle in the form of a circle. It is also a manifestation of the nonlinear photorefractive damping. With a further increase in the PR SW intensity the limit cycle shrinks to a point, turning into a stable focus ($\partial H_y/\partial x|_{x=0} = 10^{10}$, Fig. 2d). Under these conditions, the dark PRC intensity in

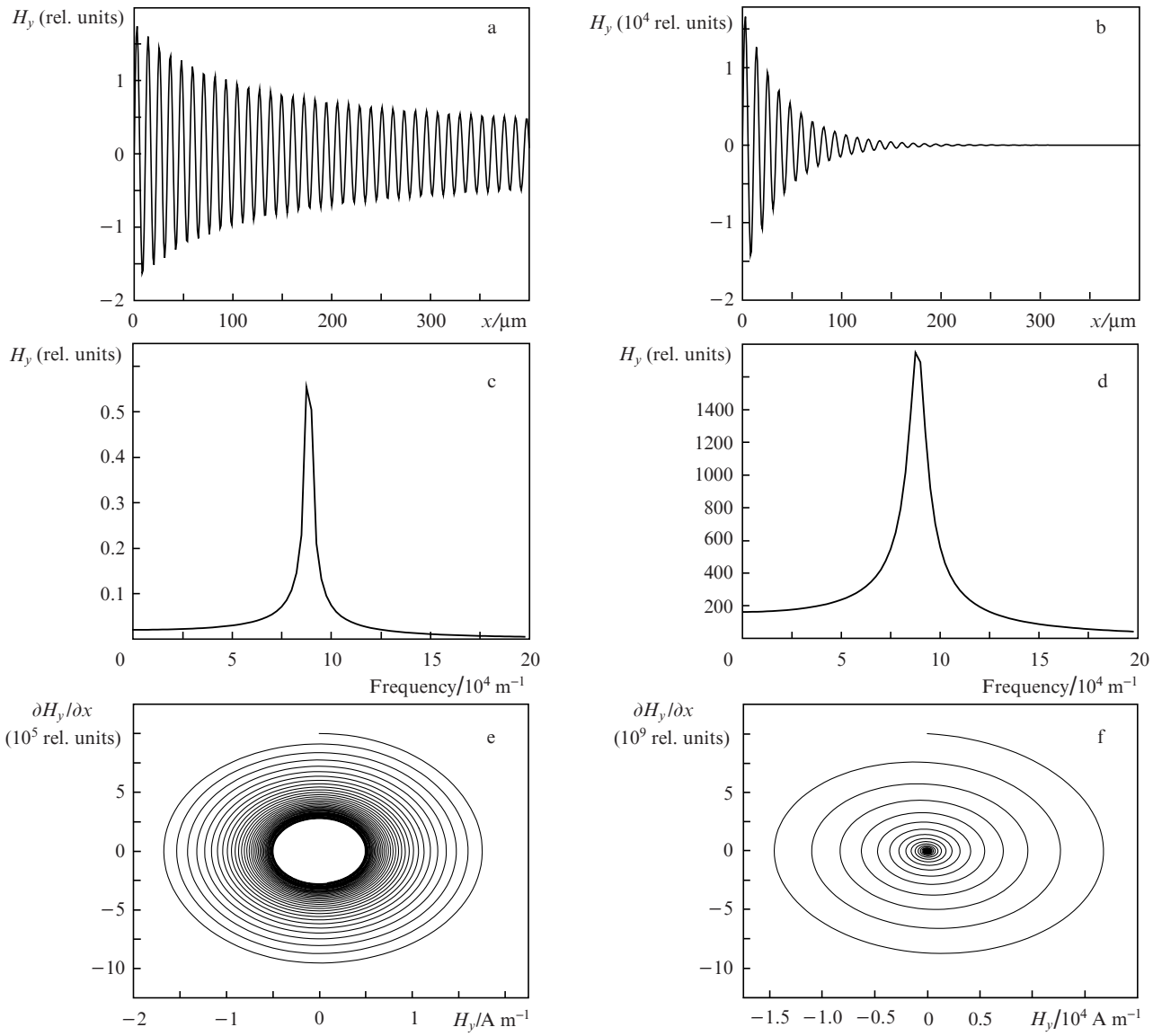

Figure 2. Distribution of the magnetic field amplitude of the TM wave $H_y(x)$ in the PR SW cross section (a, b), Fourier spectrum of spatial harmonics $H_y(x)$ (c, d) and phase trajectories of the PR SW (e, f) for $\partial H_y/\partial x = 10^6$ (a, c, e) and 10^{10} (b, d, f).

equation (8) can be neglected, and it transforms into equation (9).

Figures 3a, b show the cross-sectional distributions of the component $E_y(x)$ of the electric vector amplitude of the nonlinear TE-polarised PR SW for the boundary condition $\partial E_y/\partial x|_{x=0} = 10^8$. In calculations, the angle α between the direction of the light propagation and the crystal face that is perpendicular to the optical axis was 0.002 and 0.02 rad, the electro-optic tensor component of the SBN was $r_{13} = 47$ pmV^{-1}. In this range of the angles, the cross-sectional distribution of the component of the electric vector amplitude of the nonlinear TE-polarised PR SW also has the form of oscillations, damping in the PRC volume, whose period depends on the PR SW intensity and the angle of incidence α. The value of the first maximum $E_y(x)$ is inversely proportional to α. At $\alpha = 0.002$ rad (Fig. 3a), the value of the first maximum is equal to ~1600 at the PRC face, whereas at $\alpha = 0.02$ rad (Fig. 3b), it decreases by almost an order of magnitude – to about 180. The values of α and $\partial E_y/\partial x|_{x=0}$ equally determine the type of distribution of the PR SW amplitude, which is the larger, the smaller the angle α, and the higher the derivative $\partial E_y/\partial x|_{x=0}$. Thus, the nonlinear TE- and TM-polarised PR SWs qualitatively have the same form, despite the fact that the electro-optic tensor components for these waves differ by five times.

Above, we considered the cases when the PR SW amplitude distributions are solutions of the nonlinear equation (8) and correspond to the case of complex roots of the characteristic equation of the linear equation (9), because the solutions for both equations have the form of oscillations damping over the crystal thickness. For the SBN PRC, this is realised when $\alpha \geqslant 0.005$ rad. In the angular range $0.0002 \leqslant \alpha \leqslant 0.005$ rad, the discriminant sign of the characteristic equation of the linear equation (9) changes and its roots become real. Figures 3c, d show the amplitude distributions of the TM-polarised PR SWs for the specified range of angles α (on the PRC surface $\partial H_y/\partial x|_{x=0} = 10^8$). Aperiodic behaviour of PR SW amplitude oscillations in the cross section (Fig. 3c) changes to damped (Fig. 3d). When the discriminant of the characteristic equation is equal to zero, the PR SW amplitude distribution has the form of oscillations with critical damping. In this case,

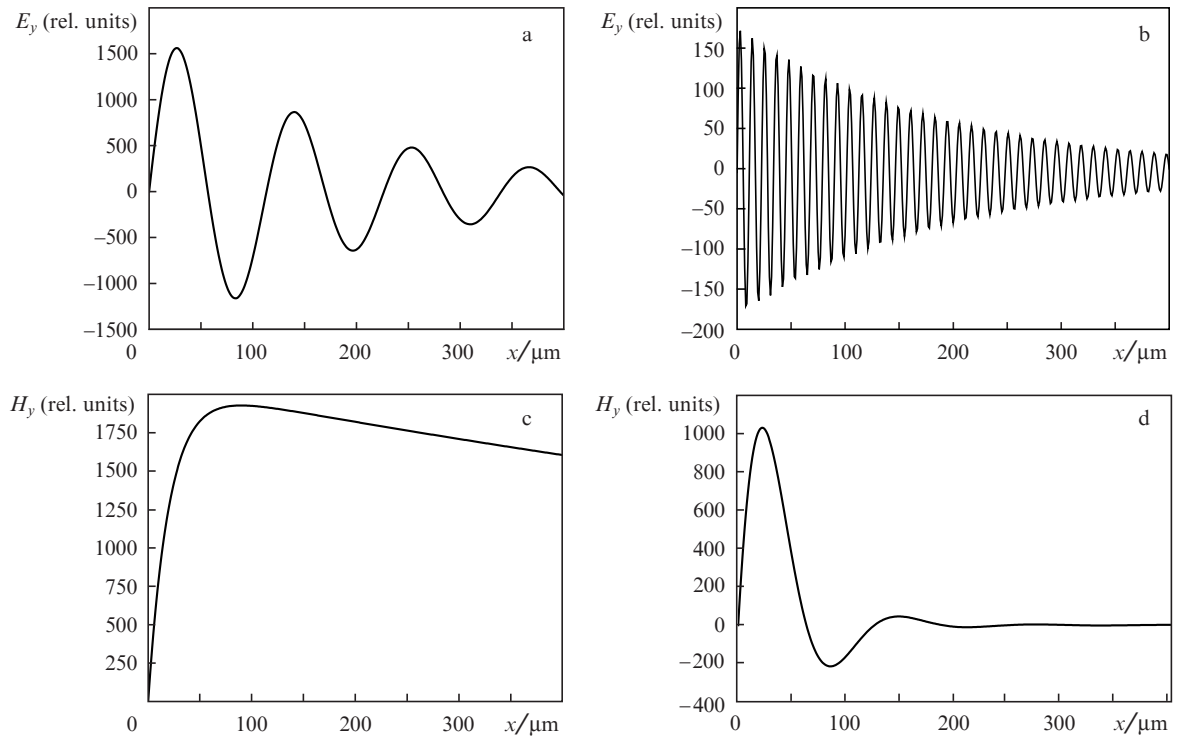

Figure 3. Distribution of the electric (a, b) and magnetic (c, d) field amplitudes of PR SWs with the TE- and TM-polarisations, respectively, in the cross section for the angles α of the wave incidence on the SBN crystal face 0.002 (a, d), 0.02 (b) and 0.0002 (c).

the highest degree of PR SW localisation is achieved at the PRC surface.

If the parameter $Q_{\mathrm{TE,TM}} = (n_{\perp,\parallel} P_{\mathrm{TE,TM}} \sin\alpha)^2 = 0$, equation (8) has a special solution: $V(u) = G(1 - e^{-u})$. It corresponds to the case $\alpha = 0$, i.e., the wave vector of light wave, $\boldsymbol{k}_0$, is parallel to the interface between the media. Under these conditions, the nonlinear PR SW is unstable, radiation is not localised in the surface layer, and the PR SW amplitude becomes non-negligibly small deep inside the PRC.

The PR SW propagation is accompanied by the appearance of the crystal electric field in the surface PRC layer [1–3], which, in turn, changes the refractive index. Assuming that the PR SW amplitude is the solution to the linear equation (9), and the intensity distribution at the crystal surface is modelled by the expression $I \sim 1 - \cos(K_{\mathrm{d}} x)$, the refractive index distribution in a photorefractive diffraction grating can be written as

$$\delta n(x) = -AE^{\mathrm{sc}}(x) = AK_{\mathrm{d}}(k_{\mathrm{B}}T/\mathrm{e})\cot(0.5K_{\mathrm{d}}x),\ I_0 \gg I_{\mathrm{d}}, \quad (12)$$

where $A_{\mathrm{TE,TM}} = 0.5 n_{\perp,\parallel}^3 r_{33,13}$; $K_{\mathrm{d}}^{\mathrm{TE,TM}} = 2\pi/\Lambda = 2k_0 n_{\perp,\parallel} \sin\alpha$ is the modulus of the photorefractive diffraction grating vector and Λ is the grating period. Analysis of expression (12) shows that, in the direction that is perpendicular to the interface, the crystal electric field is oscillating at a negative value of the discriminant of the characteristic equation. The period of spatial oscillations of the crystal field is twice smaller that the period of spatial oscillations of the PR SW amplitude in accordance with (6). Equation (12) also implies that the amplitude of the transverse spatial oscillation of the crystal electric field and the 'photorefractive' index of refraction in the limit of a high-intensity nonlinear PR SW become singular.

Figure 4 shows the distribution of the photoinduced crystal electric field and refractive index as functions of the angle α. The dependences were obtained by substituting the solution of equation (8) into (6) and (2), which determine the strength of the diffuse crystal electrical field in the surface PRC layer and the distribution of the refractive index, arising upon PR SW propagation. When the PRC nonlinearity is weak (Fig. 4a), the crystal field amplitude is 700 V m^{-1}; with increasing nonlinearity, it consistently varies from 10^4 (Fig. 4c) to 10^6 V m^{-1} (Fig. 4b); in accordance with that, the amplitude of the groove of the emerging phase diffraction grating increases from 10^{-6} to 10^{-3} (Table 1).

Thus, propagation of the nonlinear PR SW is accompanied by the formation of a refractive index grating with high diffraction efficiency. This grating can change the conditions of the wave propagation in the surface layer of the SBN. The results of calculations (Fig. 4) show that the increase in the nonlinear diffusion photorefraction, which occurs both with decreasing the angle of incidence α and with increasing the intensity of the light wave, leads to the fact that the sinusoidal profile of the phase diffraction grating transforms into that consisting of δ-functions with alternating sign, which are periodically spaced in the direction of the optical axis of the crystal. In this case, the positions of δ-functions are far ahead of

Table 1. The characteristic values of the parameters of the photorefractive diffraction grating arising in the PRC upon the PR SW propagation.

E_x^{sc}/V m^{-1}	$\partial H_y/\partial x\|_{x=0}$ (rel. units)	$\delta n/10^{-5}$	α/rad
700	10^5	0.1	0.005
13000	10^6	1.9	0.005
1300000	10^8	190	0.003
1300000	10^8	190	0.001

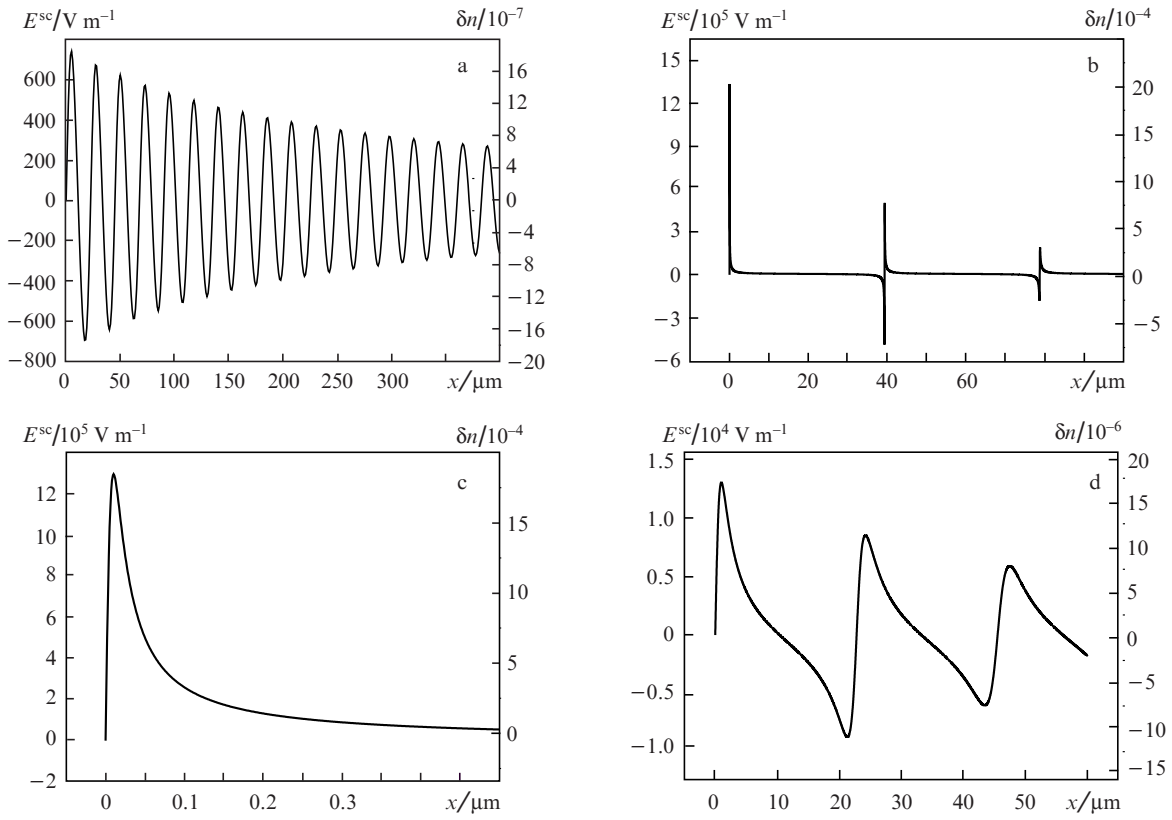

Figure 4. Distribution of the crystal field and the photorefractive index in the SBN at $\partial H_y/\partial x|_{x=0} = 10^5$ and $\alpha = 0.005$ rad (a), $\partial H_y/\partial x|_{x=0} = 10^8$, and $\alpha = 0.003$ rad (b), $\partial H_y/\partial x|_{x=0} = 10^8$ and $\alpha = 0.001$ rad (c), and $\partial H_y/\partial x|_{x=0} = 10^6$ and $\alpha = 0.005$ rad (e).

the positions of the corresponding extremes of the weak sinusoidal diffraction grating by $\pi/2$, which is in qualitative agreement with (12).

4. Conclusions

(i) We have shown that the nonlinear TE- and TM-polarised PR SWs with the diffusion-type nonlinearity are the solutions of the same equation for dimensionless variables found in the required way.

(ii) We have determined the phase trajectories of the nonlinear PR SWs for the PRC with the diffusion-type nonlinearity.

(iii) We have established the form of the photorefractive diffraction grating, whose occurrence in the surface PRC layer is due to the PR SW propagation. We have shown that the refractive index amplitude of the diffraction grating is defined by the propagation constant β, i.e., the grazing angle of the beam, its intensity, polarisation, and can reach $\sim 10^{-3}$.

Acknowledgements. The authors thank V.A. Sychugov and B.A. Usievich for their help. This work was supported by the Russian Foundation for Basic Research (Grant No. 10-02-01389).

References

1. Petrov M.P., Stepanov S.I., Khomenko A.V. *Photorefractive Crystals in Coherent Optical Systems* (Berlin: Springer-Verlag, 1991; St Petersburg: Nauka, 1992).
2. Vinetskii V.L. *Dinamicheskaya golografiya* (Dynamic Holography) (Kiev: Naukova Dumka, 1983).
3. Kukhtarev N.V., Markov V.B., Odulov S.G., Soskin M.S., Vinetskii V.L. *Ferroelectrics*, **22**, 949 (1979).
4. Christodoulides D.N., Carvalho M.I. *J. Opt. Soc. Am. B*, **12**, 1628 (1995).
5. Garcia Quirino G.S., Sanchez-Mondragon J.J., Stepanov S.I. *Phys. Rev. A*, **51**, 1571 (1995).
6. Zhang T.H., Ren X.K., Wang B.H., et al. *Phys. Rev. A*, **76**, 013827 (2007).
7. Aleshkevich V., Kartashov Ya., Egorov A. *Phys. Rev. E*, **64**, 056610 (2001).
8. Garcia Quirino G.S., Sanchez-Mondragon J.J., Stepanov S.I., Vysloukh V.A. *J. Opt. Soc. Am.*, **13**, 2530 (1996).
9. Zhang T.H., Yang J., Kang H.Z., et al. *J. Mod. Optic*s, **54**, 1165 (2007).
10. Yariv A., Yeh P. *Optical Waves in Crystals: Propagation and Control of Laser Radiation* (New: Wiley, 1984; Moscow: Mir, 1987).
11. Landau L.D., Lifshitz E.M. *Electrodynamics of Continuous Media* (Oxford: Pergamon Press, 1984; Moscow: Nauka, 1982).
12. Born M., Wolf E. *Principles of Optics* (London: Pergamon, 1970; Moscow: Nauka, 1973).
13. Zhang T.H., Ren X.K., Wang B.H., et al. Phys. Rev. A, 76, 013827 (2007).
14. Sedov L.I. *Similarity and Dimensional Methods in Mechanics* (New York: Acad. Press, 1959; Moscow: Nauka, 1977).
15. Garcia Quirino G.S., Sanchez-Mondragon J.J., Stepanov S.I., Vysloukh V.A. *J. Opt. Soc. Am.*, **13**, 2530 (1996).
16. Bessekerskii V.A., Popov E.P. *Teoriya sistem avtomaticheskogo regulirovaniy*a (Theory of Automatic Control Systems) (Moscow: Nauka, 1972).